2.11 BIOMEDICAL APPLICATIONS OF LIBS

Steven J. Rehse

ABSTRACT

The use of laser-induced breakdown spectroscopy (LIBS) as a biomedical diagnostic tool is rapidly gathering significant attention due to successful demonstrations of its utility in a surprisingly broad range of applications. Broadly speaking, these applications can be divided into two categories: those which aim to quantify or monitor elemental concentrations in medical or biomedical specimens and those that use unique elemental compositions to rapidly identify or classify specimens. In this chapter, we will review recent progress in the application of LIBS in several broad classes of biomedical diagnostics, including the analysis of hard/calcified tissues; the analysis of soft tissues; the analysis of biomedical specimens; the identification/classification of agents causing human disease; and laser-guided surgery.

1. INTRODUCTION.

1.1 Motivation

Lasers are one of the most important tools available in modern medicine. The applications of lasers in medicine are extremely disparate and exploit all of the various properties intrinsic to laser light, such as monochromaticity, focusability, high power density or fluence, and the ability to deliver energy in ultrashort pulses. Most of these applications involve the interaction of the laser's electromagnetic radiation with cells or tissues in some way. In the medical field it is common to define three different regimes of interactions depending on the energy density of the delivered laser light and the time duration over which the energy is deposited within the tissue. These three regimes are loosely defined as: photocoagulation, photovaporization (or photodisruption), and photoablation.[1,2]

Photovaporization and photoablation procedures which commonly use pulsed lasers of nanosecond or shorter pulse duration have achieved great acceptance in a wide variety of medical procedures. Although it is not our intent to summarize all of these here, a short list of the procedures commonly performed include corneal refractive surgery (LASIK),[3] laser angioplasty,[4,5] laser hair removal,[6] laser tattoo removal,[7] and laser surgery.[8,9] The advantages proffered by the use of the laser include the ability to perform *in vivo* procedures endoscopically,[10,11] comparatively lower complication rates,[3] and treatment areas which exhibit high precision with no thermic damage, little depth effect, and no delay of healing processes.[8]

In this medical context, a laser-induced breakdown spectroscopy (LIBS) measurement is a photovaporization or photoablation event in which the resulting optical emission is utilized for some useful diagnostic purpose. It is significant that although photoablation procedures are common in laser medicine, the real-time analysis/feedback that can be provided by an optical analysis of the ablation event (performing LIBS) is not currently utilized or exploited. It is this real-time control of the medical procedure, or the ability to immediately obtain diagnostic information, that is the greatest advantage that LIBS brings to the biomedical sciences and the practice of medicine.

A number of excellent review articles and review chapters already exist describing the application of LIBS techniques and instrumentation in the biomedical/medical field.[12,13,14,15] It is the goal of this chapter to describe the applications of LIBS in a broader medical context for the interested non-LIBS medical practitioner or biomedical investigator and to provide a completely up-to-date survey of the field, with a specific emphasis on peer-reviewed literature that can be relatively easily obtained by such a practitioner and should be broadly accepted by the wider medical community.

1.2 Definition and categorization of biomedical LIBS applications

Before reviewing the relevant literature, it is necessary to construct a working definition of biomedical LIBS applications. Firstly, from this point on, we will utilize the work "biomedical," but it is to be understood that this directly implies "medical" applications as well. Secondly, we will limit our review to strictly "biomedical" applications (applications directly affecting human health and wellness) as opposed to the broader category of "biological" applications, which include analyses of living and/or biological targets such as plant tissues, animal tissues, soil samples, etc. Lastly, we will further restrict the conversation by omitting those applications that involve human health indirectly but cannot specifically be considered "medical" in nature. A short list of such applications, which have been widely described elsewhere, includes: the analysis of water contamination to determine its safety for human consumption; the analysis of foods, plants, or beverages so as to determine their nutritional composition; the *in situ* detection of biological aerosols (which is more appropriately described in the context of sensing, security, or environmental monitoring); and the application of LIBS in the monitoring of pharmaceutical and pharmaceutical coatings fabrication.

With this definition in place, the biomedical applications of LIBS can be classified into two broad categories according to the ultimate goal of the analysis. These two categories are: (1) the use of LIBS as an elemental assay and (2) the use of LIBS for the classification of an unknown target. In the first category, the practitioner may use the LIBS elemental spectrum to measure or quantify the concentration or change in concentration of a specific element or elements present in a biomedical specimen to diagnose, monitor, or predict a disease state. An example of this is the use of the intensity of a specific calcium emission line to discriminate healthy from carious dental tissue (described in detail in section 2.3 below). In the second category, the LIBS elemental spectrum is used as a unique "signature" or "fingerprint" to rapidly classify the biomedical specimen (perhaps using a precompiled library of reference specimens) to diagnose, monitor, or predict a disease state. In this category of applications, the absolute concentrations or quantities of specific elements are unimportant for the diagnosis and are typically not measured. An example of this is the use of LIBS spectra to discriminate pathogenic from non-pathogenic bacteria (described in detail in section 5.2 below). This concept of the two categories which utilize the LIBS spectrum in different ways is shown in Figure 1.

Although this chapter is not organized by these two categories, it is important to remember that each described application falls into one category or the other and the practitioner is advised to keep the intent of the LIBS analysis in mind, as this can and will impact many experimental parameters, such as the choice of laser, spectrometer, and data

analysis technique. In fact, the chapter will describe several broad classes of biomedical applications, including: the analysis of hard/calcified tissues; the analysis of soft tissues; the analysis of biomedical specimens; the identification of agents causing human disease; and the use of LIBS during laser-guided surgery.

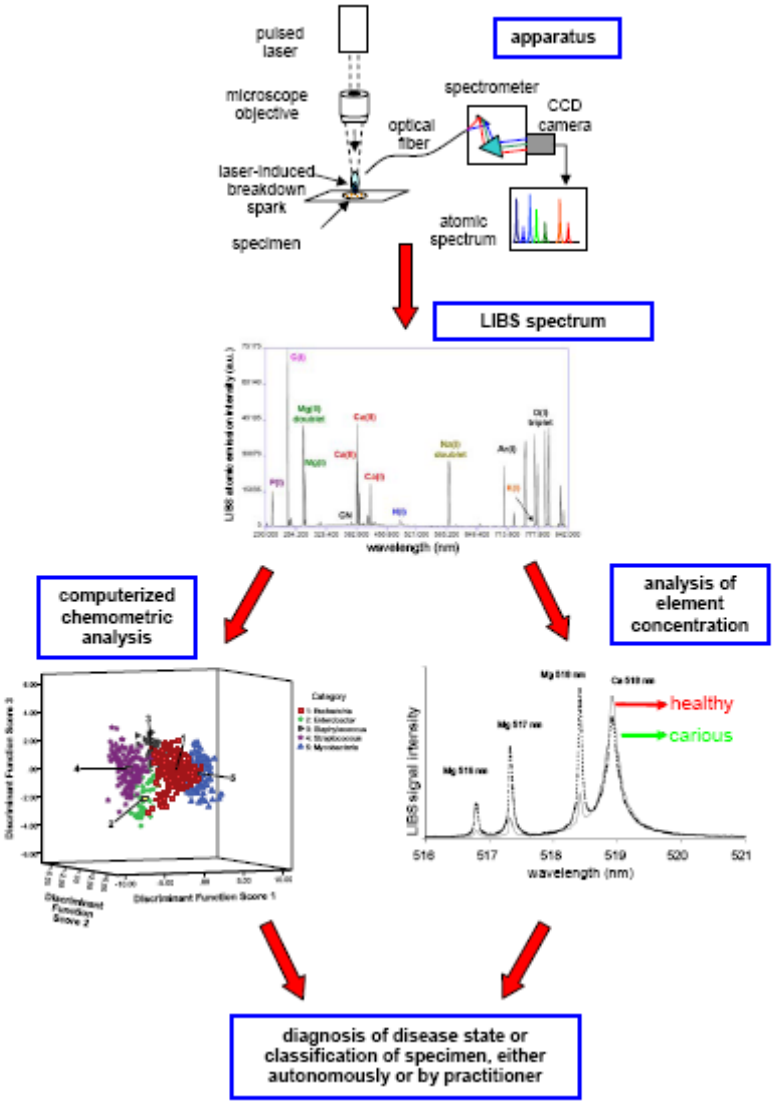

Figure 1. An illustration of how a LIBS analysis of a biomedical specimen can be performed in one of two ways. In both cases, a specimen is interrogated via LIBS either *in vivo* or *ex vivo* and a spectrum of elemental emission lines is obtained (*top, adapted from ref. 14*). The LIBS spectrum is then either analyzed with a multivariate chemometric analysis and compared to a pre-existing library of similar spectra for classification (*left, adapted from ref. 103*) or specific individual lines are monitored to quantify an elemental concentration indicative of some underlying pathology or disease state (*right, adapted from ref. 17*). In both cases this diagnosis may be made autonomously via computer analysis, via observation by a medical practitioner, or some combination of the two (*bottom*).

2. ANALYSIS OF HARD/CALCIFIED TISSUES.

2.1 Introduction

It was recognized early on that pulsed lasers effectively ablated both hard and soft tissues, with the threshold fluence for laser-induced breakdown of hard tissues (such as bone or enamel) being lower than the threshold for soft tissue ablation, the effect being somewhat dependent on pulse duration.[16] Since that time numerous studies have been conducted on a variety of tissues of both types. There are numerous advantages to performing analyses on hard tissues including: the ease with which breakdown can be achieved on the hard, opaque, mineralized surfaces, the robustness of the specimen after removal from the patient, the high concentrations of elements easily observed in LIBS plasmas (such as Ca and Mg) in such tissues, and the ability to easily cross-section specimens. In this section, we will describe experiments conducted on the hard or calcified tissues, dental tissues, urinary stones and calculi, and fingernails.

2.2 Calcified Tissues

Important diagnostic information can be obtained from calcified tissues via the LIBS technique. Assays of the observed elemental concentrations can provide information about the tissue's age, the environmental conditions of its growth (perhaps related to the patient's geographic location), the dietary influences of the person from which the sample was obtained, and the accumulation of potentially toxic elements.[15] In 2001, Samek et al. utilized a 1064 nm nanosecond Nd:YAG laser to monitor strontium concentration in specimens of human bone (tibia and femur).[17] Concentrations in the range of 100's of ppm were measured and confirmed via atomic absorption spectroscopy. The authors also demonstrated two dimensional mapping of strontium in cross-sections of a human tibia with 1 mm resolution.

In a 6 m standoff experiment in 2009, Hrdlička et al. demonstrated that LIBS performed with a 532 nm nanosecond laser is sufficiently sensitive at that distance to monitor the concentration of both major (P and Mg) and minor (Na, Zn, and Sr) elements in a bone sample. They were then able to determine the radial distribution of those elements in the cross-sectioned bone sample.[18]

2.3 Dental studies (tooth enamel, dental caries)

In a series of papers spanning several years, a group of researchers from the University of Brno in the Czech Republic and the University of Wales-Swansea in the United Kingdom extensively studied the use of LIBS in a variety of dental applications, summarized here.[17,19,20,21] Using nanosecond 1064 nm laser pulses on a variety of removed and cross-sectioned dental tissues, they were able to show that by using LIBS to quantify and monitor changes in the concentrations of major elements (such as Ca and Mg) and minor elements (such as Ag, Al, Ca, Cr, Hg, K, Mg, Mn, Na, Ni, P, Sn, Ti, and Zn) at the level of a few tens of parts per million in real-time, clinically relevant information can be obtained and utilized as a feedback diagnostic by the dental practitioner. Particular experimental emphasis was placed on two components of the tooth tissue which made excellent LIBS targets: the surface enamel of the tooth, which is the hardest substance in the body (composed of 95% hydroxyapatite $Ca_{10}(PO_4)_6(OH)_2$, 4% water, and 1% organic matter) and the dentine which lies under the enamel (composed of 70% hydroxyapatite, 20% organic matter, and 10% water.)[20] From their results, they concluded that it is possible to establish a link between elements detected in toothpastes, tooth fillings, and other restorative compounds with those present in the

tooth and also to relate the spatial distribution of such elements to their migration and accumulation in the tooth due to exposure to those dental materials.

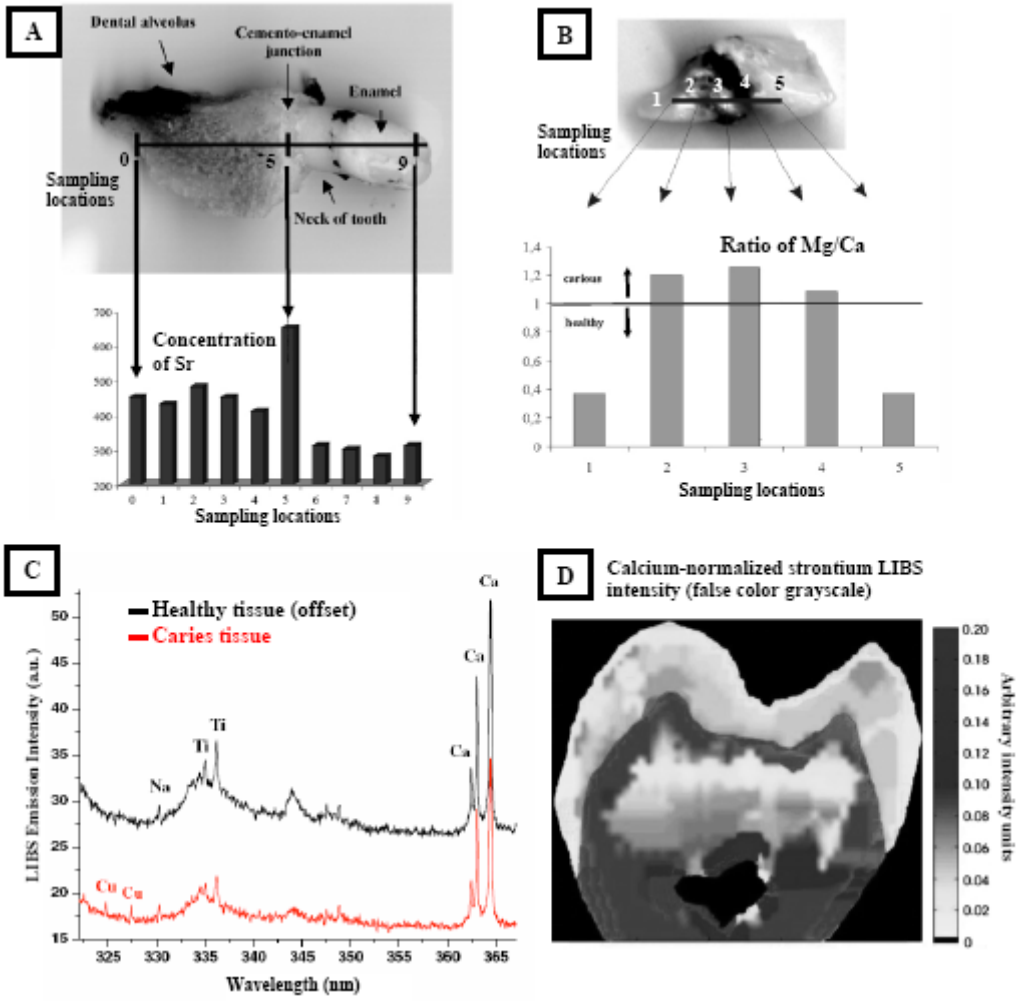

Figure 2. The application of LIBS to the analysis of dental tissue. (*A*) Point sampling of a tooth reveals changes in the concentration of strontium as a function of location throughout the tooth *(adapted from ref. 17)*. (*B*) Point sampling of a tooth across a region of carious tissue reveals the ratio of Mg/Ca can be a reliable indictor of tooth decay (*adapted from ref. 17*). (*C*) The LIBS spectrum reveals multiple elemental changes in the caries tissue relative to the healthy tissue, including the concentrations of Cu, Ti, and Ca (*adapted from ref. 23*). (*D*) A two-dimensional false color surface map of a tooth's strontium concentration. The Sr LIBS emission was normalized to a strong emission line of calcium to improve shot-to-shot reproducibility (*adapted from ref. 26*).

Most importantly, Samek et al. were able to discriminate regions of tooth decay (caries tissue or carious tissue) from healthy tissue via one-dimensional line scans and two-dimensional spatial mapping of elemental concentrations. They did so by observing a reproducible difference in the LIBS spectrum obtained from caries and healthy tooth material via a decrease in calcium and phosphorus concentrations. The most frequent pathological condition of teeth is decay or caries infection, in which the enamel becomes demineralized and the hard enamel becomes more porous.[21] By quantifying those elemental changes, healthy tooth material could be distinguished with high spatial

resolution. The authors concluded that by using a computerized pattern recognition (chemometric) algorithm, the identity (caries vs. healthy) of an unknown tooth sample could be determined in real-time. This is shown in Figure 2.

In 2008 Thareja et al. using a 355 nm nanosecond LIBS system also observed spectral changes consistent with the presence of caries tissue.[22] They measured a dramatic variation in the relative concentrations of Ca, Sr, and Na in carious tooth tissue relative to healthy tissue. This variation was the result of calcium bound to the hydroxyapatite being washed out of the caries tissues and being replaced by other elements. The conclusion reached by these groups is that LIBS has the potential to become a useful tool for *in vivo* / *in vitro* caries identification during a drilling or cleaning process with a spatial resolution on the order of 100-200 μm and a depth resolution of approximately 10 μm.[21]

In 2011 Singh and Rai reached the same conclusion and also observed a decrease in the concentration of titanium (a common additive to toothpaste in the form of TiO_2 and a common element in dental implant material) and an increase in the concentration of Cu (absorbed during normal eating, drinking, and breathing) in caries-affected tissues relative to healthy dental tissue.[23] This is shown in Figure 2.

Abdel-Salam et al. have shown that not only can the elemental composition of a tooth be measured, but that enamel surface hardness can be determined.[24] By monitoring the ratio of CaII/CaI and MgII/MgI, they were able to quantify elemental differences and thus classify specimens of human tooth enamel obtained from two dynasties of ancient Egyptians and from two populations of modern man.[25] As well, these authors investigated the dependence of the classification on the use of a single-pulse or double-pulse LIBS technique and also on the use of nanosecond versus picosecond laser pulse durations. In a related study, Alvira et al. demonstrated that LIBS analysis of trace elements in teeth can be an effective tool for use in anthropology and paleontology by measuring strontium and magnesium levels in dentin and enamel in tooth samples from Neolithic, middle age, and modern Homo sapiens teeth.[26] They also constructed two-dimensional surface distribution maps of Ca-normalized Mg and Sr concentrations, and showed that these can be interpreted in the context of early nutrition, seasonality, and residential mobility. This is shown in Figure 2.

2.4 Stones and calculi

A calculus is a stone (a concretion of material, usually mineral salts) that forms in an organ or duct of the body. The most common stones are gallstones, urinary bladder stones, and kidney stones.[27] Upon removal from the body, an elemental analysis of a stone's composition is often a first step in a diagnosis of patient pathology.[28] It has even been suggested that the analysis of urinary calculi can be helpful in providing complementary information on human exposure to mercury.[29] Methods that have commonly been used for such analyses include inductively-coupled plasma atomic emission spectroscopy (ICP-AES), graphite furnace atomic absorption spectroscopy (AAS), proton-induced X-ray emission (PIXE), neutron activation analysis (NAA), X-ray fluorescence (XRF), scanning electron microscopy (SEM) with energy dispersive x-ray fluorescence microanalysis, and laser ablation inductively-coupled plasma mass spectrometry (LA-ICP-MS).[30,31,32,33,34] All of these analytical techniques require time and labor-intensive expertise to perform.[31] Also, many of them provide no spatial

information about the distribution of the elements within the stone, which can be important since it has been shown that such stones can consist of lamellar structures with at least two types of layers on the scale of 10's to 100's of microns.[35,36] Clearly the sensitive elemental qualification provided by the LIBS spectrum along with its excellent resolution on the proper length scales suggest that LIBS could be a powerful tool for the rapid and inexpensive analysis and elemental mapping of stone etiology.

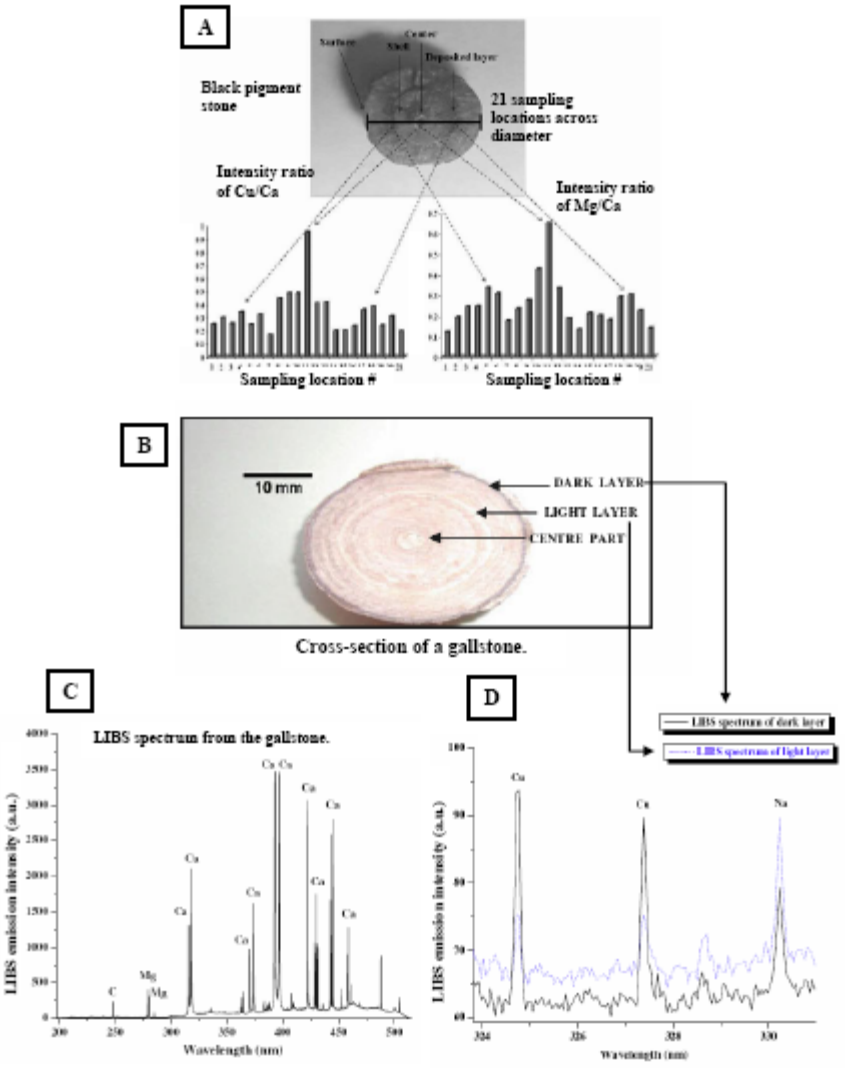

Figure 3. Elemental and mineral analyses can be conducted on cross-sectioned calculi including gallstones, urinary stones, and kidney stones. (*A*) 21 LIBS measurements were performed across the diameter of a cross-sectioned black pigment gallstone. Evidence of increased Cu and Mg concentrations in the core nucleation site were observed (*adapted from ref. 28*). (*B*) A cross-sectioned 3.5 cm gallstone exhibiting concentric dark and light layers. (*C*) The LIBS spectrum of the stone exhibited excellent signal to noise and indicted the presence of calcium, magnesium, copper, iron, sodium and potassium. (*D*) An analysis of different colored layers indicated quantifiable differences between the dark and light layers particularly a decrease in the quantity of Cu, and to a lesser extent Na, in the light layer. (*B, C, D adapted from ref. 38).*

Singh et al. demonstrated that the LIBS spectrum from 200-90 nm obtained with nanosecond 532 nm pulses on surgically removed gallstones could be used to classify the

stones as cholesterol stones, black pigment stones, or mixed stones.[27,28] As well, they performed a quantitative analysis of trace metal elements with results in agreement with inductively coupled plasma atomic emission spectroscopy (ICP-AES) measurements and recorded single-shot LIBS spectra from different points on the cross section to study the variation of constituents from the center to the surface. This is shown in Figure 3. In a similar study they measured the *in situ* elemental spatial distribution of kidney stones and made a quantitative estimation of the concentrations of Cu, Mg, Zn, and Sr in different parts of the stones.[37] A spatial analysis of cholesterol stones was also performed, demonstrating that the light elements, such as hydrogen, carbon, and oxygen (which can be difficult for other techniques such as XRF to detect), could be easily detected by LIBS in these stones. They concluded that Cu and Mg play important roles in the nucleation and formation of the stones on the basis of their distribution from the center to the surface. In a related study, these authors used the atomic spectral lines and the observed molecular bands (such as CN and C_2) to characterize the different layers seen in the gallstones.[38]

To allow the efficient rapid identification or classification of unknown calculi, Anzano et al. investigated different algorithm strategies for urinary calculi classification.[39] Statistical correlation analysis using linear (parametric) and non-parametric (rank) correlation was used to analyze spectra obtained from kidney stones using a nanosecond microscope-coupled LIBS system (approximately 9 mJ/pulse). It was found that the best results were obtained by using the linear correlation with a spectral window between 200 and 400 nm. The authors also analyzed the elemental ratios obtained when the kidney stones were ablated with 532 nm nanosecond pulses (115 mJ/pulse) and the entire emission spectrum was detected with an Échelle spectrograph with an ICCD camera (no microscope). They concluded that both algorithms and instruments provided reliable strategies for urinary-calculi identification.

2.5 Fingernails

Fingernails and toenails are made of a tough protein called keratin.[40] The concentration or sequestration of trace elements in the nails over conveniently long time scales [41,42] as well as the general relationship between nail mineral/elemental composition and bone health specifically,[43] and total health more generally,[44] makes them an ideal target for LIBS analysis.

Hosseinimakarem et al. used 1064 nm nanosecond pulses to obtain LIBS spectra from removed cleaned nails.[45] The elements detected in the emission spectra were Al, C, Ca, Fe, H, K, Mg, N, Na, O, Si, Sr, Ti as well as CN molecular emission. Using a discriminant function analysis (DFA), the authors were able to discriminate among specimens from different genders and age groups. It was noted that the number of samples in the study and their distribution was not sufficient to generate a truly statistically significant analysis. Intriguingly, it was observed that there was an agreement between elevated levels of potassium and sodium in the fingernails (as determined by the LIBS spectrum) and hyperthyroidism and high blood pressure as indicated by self-reporting and also as measured in blood test results. This is intriguing because a potassium deficiency is one of the symptoms of hyperthyroidism and a high level of an element in the hair or in nails may indicate a depletion of that element in the body.[45]

In a related work, Bahreini et al. also utilized a DFA of LIBS spectra to discriminate healthy subjects and those suffering from hyperthyroidism, an illness of the thyroid associated with an overproduction of the thyroid hormone, and hypothyroidism, a disorder associated with underactivity of the thyroid gland.[46] The DFA was performed on emission line intensities and ratios of intensities. Efficient discrimination was observed between nails from subjects with these conditions, with the K/Ca and Na/Ca ratios providing the most efficient discrimination.

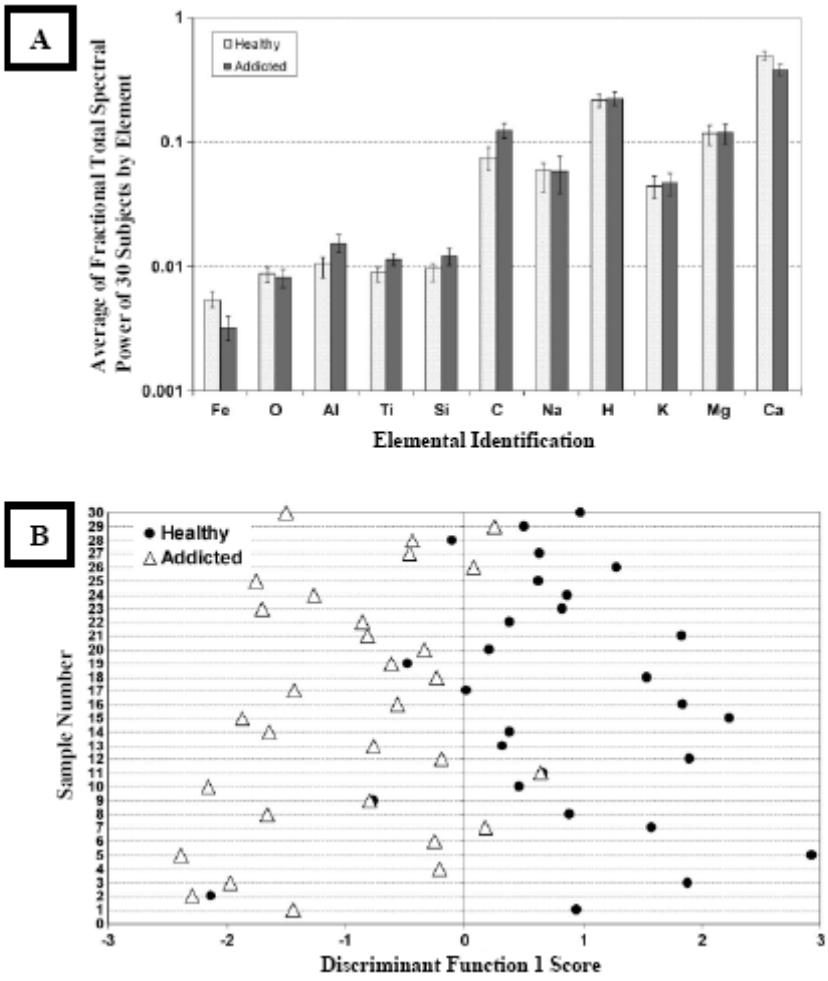

Figure 4. Elemental analysis of human fingernails can provide important indicators of health and reveal conditions such as hyperthyroidism and addiction to opiates. The fingernails of 30 healthy control subjects and 30 opium addicted subjects were tested. (*A*) The strength of LIBS emission from 11 elements was used to construct a spectral fingerprint. The fraction of the total spectral power (the sum of all observed emission intensities) due to each element is shown for both groups, averaged for all 30 subjects in the group. (*B*) A discriminant function analysis of the intensities of 41 observed spectral lines from these 11 elements was used to discriminate healthy from opium-addicted subjects. In this DFA, 23 out of 30 healthy subjects (solid circles) and 21 out of 30 addicted individuals (triangles) were correctly classified in a cross-validated test. (*A and B adapted from ref. 50).*

In what may be the first analysis of pathological nail conditions, Hamzaoui et al. in 2011 used a 532 nm nanosecond LIBS system to simultaneously measure the relative

concentrations of Ca, Na, and K in healthy and pathological nails diagnosed with the fungal infection onychomycosis.[47] LIBS spectra were acquired from the upper and inner faces of the nails, and in the case of the pathological nails, spectra were taken from both yellow and brown regions of the inner face. Intensities of Ca and Na emission lines, normalized by the 766.49 nm emission line of K, were found to discriminate the healthy nails from the pathological nails.

It has been recognized that due to the accumulation and sequestration of elements in the nail as a function of time and exposure, the nail may be used as a suitable biological sample in toxicological analyses for forensic purposes.[48,49] To this end, Shadman et al. used 1064 nm nanosecond pulses to perform LIBS in a helium environment on 60 fingernails belonging to healthy and opium addicted subjects.[50] It was observed that the concentrations of Fe, Ca, Al, Si, Ti, O, and C were different in the two groups while concentrations of Mg, K, H, and Na were almost equal between both groups. Fe and Ca were elevated in healthy subjects and Al, C, Ti and Si were elevated in samples from addicted subjects compared to the healthy subjects. A DFA was performed on 41 observed spectral lines and it was able to correctly classify 23 out of 30 healthy subjects and 21 out of 30 addicted subjects in a cross-validated test. Five similar tests resulted in an average sensitivity of approximately 72%. No externally validated test – where samples not included in the construction of the DFA model are tested - was performed in this analysis. This is shown in Figure 4.

3. ANALYSIS OF SOFT TISSUES.

3.1 Introduction

Compared to the calcified tissues discussed in section two, performing LIBS on soft tissues can involve significant difficulties, not the least of which are a paucity of sample, difficulty in obtaining well-defined representative tissue cross-sections, the varying effect of tissue hydration (depending on whether the tissue has been preserved or not), and sample heterogeneity (in both the lateral and depth dimension).

Despite this, significant work has been performed on a variety of soft tissues. In this section, the studies of these tissues are organized into the categories of organs, malignancies, and skin/hair.

3.2 Organs

One of the first studies to investigate the characteristics of optically-induced breakdown on soft tissue was performed by Loesel et al. on human corneal tissues and bovine brain tissues, both of which were comprised of approximately 75% water.[16] Samples were tested quickly after removal and were frequently sprayed with water to prevent surface dehydration. No attempt was made to perform spectroscopy on the ablated tissues or to elementally characterize the tissues tested as the authors were primarily concerned with demonstrating the usefulness of the technique in surgical operations, but they did conclude that the threshold fluence for these tissues decreased for shorter pulse durations.

One of the first reports of LIBS performed on a non-skin / non-hair soft tissue appeared in 2003 when de Souza et al. used a nanosecond 1064 nm laser system to ablate

chicken myocardium.[51] The only identifiable elemental emission observed in this LIBS plasma was from sodium, hydrogen, calcium, and magnesium. While no other conclusions were reached other than the ability to observe elemental emission, the authors postulated that the use of such a spectrum could one day lead to a new diagnostic technique for the discrimination of different tissues and even pathological conditions.

In 2007 Rehse et al. utilized an aluminum-doped agarose model to determine the sensitivity of trace aluminum detection in simulated human tissue, representing retinal tissue into which Al had leached from sapphire-substrate implants.[52] Using a nanosecond 1064 nm laser system, limits of detection on the order of 1 ppm were measured in the highly hydrated model tissue (>98% water) both with and without the use of Ca emission lines for signal normalization.

In 2008 Santos et al. investigated the use of femtosecond LIBS on sample pellets prepared from certified reference tissues including liver, kidney, muscle, hepatopancreas, and oyster.[53] This study intended to demonstrate the utility of the technique for use in a pathology laboratory on specimens after biopsy. A sample preparation protocol consisting of cryogenic grinding-assisted homogenization followed by pelletization in a 2 ton/cm^2 press without binding agents was used. Emission spectra were dominated by calcium, magnesium, and sodium (as well as molecular emissions). Emission from trace elements such as Al, Cu, Fe, K, P, Zr, and Sn was observed with detection limits at the 1 to tens of ppm limit.

In 2009 Yueh et al. obtained LIBS spectra from frozen (-20°C) specimens of chicken brain, lung, spleen, liver, kidney and skeletal muscle using a nanosecond 532 nm LIBS system.[54] Using a variety of chemometric data analysis techniques, including cluster analysis, partial least squares discriminant analysis (PLS-DA), and neural network analysis (NNA), they demonstrated that the different types of tissue samples could be efficiently differentiated and subsequent unknown tissues could be identified. The authors noted that the selection of analyte lines played an important role in achieving correct identification and that the number of spectra obtained from each sample needed to be as large as possible to improve sampling statistics.

3.3 Cancerous/malignant tissues

While the previous studies focused on the ability to identify or discriminate presumably healthy tissues, a considerable amount of work has been done to differentiate healthy tissues from malignant or cancerous tissue. In the first such study, Kumar et al. utilized a nanosecond 532 nm LIBS system to acquire spectra to distinguish normal and malignant tumor cells in histological sections of a canine hemangiosarcoma.[55] They observed that the concentration of trace elements like Ca, Na, and Mg were higher and the concentration of Cu was lower in malignant cells relative to the normal cells. These results were confirmed with inductively coupled plasma emission spectroscopy (ICPES).

In 2008 Myers et al. proposed utilizing a portable LIBS system composed of an "eye safe" erbium glass laser at 1.54 μm and a fiber spectrometer to non-invasively diagnose malignant skin tissue.[56] It was anticipated that changes in the observed quantity of calcium, relative to an unchanging quantity of aluminum, would provide a spectral marker of malignant tissue. The authors observed that great care must be taken when performing LIBS on skin samples as elemental concentrations and ratios vary with depth below the surface of the skin on the scale of ten's of μm. Nonetheless, they

reported measureable concentrations of the trace elements Al, Ca, Cu, Fe, Zn, Na, and K at the 10's to thousand's of ppm in the stratum spinosum, the stratum cornium, and the stratum basale of healthy skin on the back of the hand.

In 2009 Markushin et al. proposed a fundamentally different way of utilizing LIBS to diagnose cancerous or malignant tissues.[57] Rather than quantifying differences in elemental concentrations, they performed a sensitive detection of the ovarian cancer biomarker CA 125 by utilizing an elemental "tag." Immuno-conjugated silicon micro-particles (1.5 μm) were fabricated and incubated with agarose beads carrying CA 125 molecules. After careful washing, a LIBS-based detection of silicon in the emission spectrum indicated the presence of the ovarian cancer biomarker. Although no limit of detection was reported, in a very similar experiment performed with an Fe micro-particle assay a limit of detection of 30 ppb was determined for the model protein avidin. Subsequent studies determined a limit of detection of about 1 U (international units)/ml for CA 125 and about 11 μg/ml for the ovarian cancer biomarker Leptin, comparable to current existing enzyme-linked immunosorbent assays (ELISA).[58]

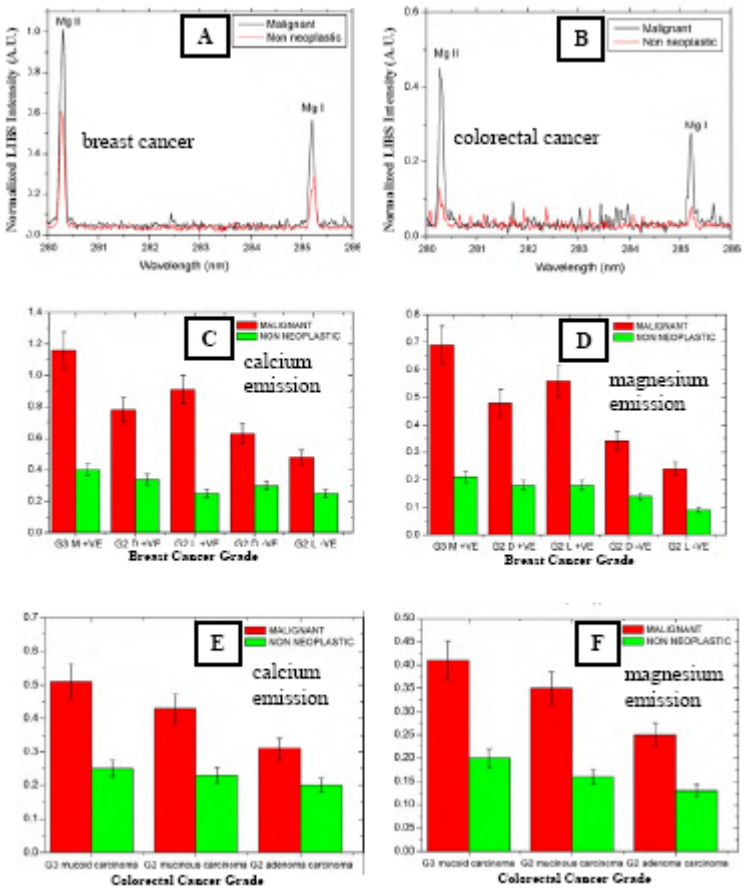

Figure 5. Elemental analysis of human tissues can reveal differences indicative of malignancies. A significant increase in the LIBS emission intensity from magnesium was observed in liquid-nitrogen-frozen tissue specimens diagnosed by a pathologist as breast cancer (*A*) and colorectal cancer (*B*) relative to non-neoplastic specimens. The measured LIBS emission intensities from the Ca II line at 373.6 nm (*C*) and the Mg I line at 285.2 nm (*D*) were significantly enhanced in multiple grades of breast cancers. The measured LIBS emission intensities from the same lines of Ca (*E*) and Mg (*F*) were also significantly enhanced in multiple grades of colorectal cancers (*adapted from ref. 59).*

In 2010 El–Hussein et al. investigated the use of LIBS for the identification/characterization of colorectal cancer and breast cancer. By detecting a significant increase in the abundance of calcium and magnesium in malignant tissues relative to the healthy tissues, discrimination was observed in 41 specimens of breast cancers of grade 2 and 3 (with various conditions of metastasis) and 32 specimens of colorectal cancers of grade 2 and 3.[59] This is shown in Figure 5. These experiments were performed with a 532 nm nanosecond Nd:YAG system under vacuum (10^{-2} Torr) in a specially designed vacuum chamber. In addition, the specimens were frozen down to −196°C. An increase in both calcium and magnesium was observed in atomic absorption spectrometry (AAS) measurements of uterine cancer tissues, where a significant increase in Ca^{2+} concentration and an insignificant increase in Mg concentration was observed when compared to non-neoplastic uterine tissues. A significant increase in Mg and the Mg/Ca ratio was reported in uterine myoma, confirming the observations of El-Hussein et al.[60]

3.4 Hair/skin

In 2000 Sun et al. investigated the use of nanosecond LIBS with 1064 nm laser light to analyze the concentration of trace elements in human skin, specifically zinc in the stratum corneum.[61] As commented by them (and references therein) trace elements in the skin, such as the metals Mg, Zn, Ca, and Fe, play important roles in skin cell biology, relating rates of cell turnover and cell metabolism, for example. Concentrations of these trace metals are therefore biomarkers for overall skin health. By applying zinc in solution prior to the removal of skin specimens, they were able to efficiently track the absorption of the metal as a function of depth through the skin to a depth of approximately 12-18 μm. By testing the skin specimens on glass slides, they were able to measure concentrations effectively to 0.3 ng/cm^2 with a calibration curve exhibiting good linearity up to 1000 ng/cm^2. The unit of "mass per unit area" rather than "concentration (in ppm)" was due to the sample preparation methodology used in the creation of their calibration curves.

Corsi et al. have investigated the use of calibration free LIBS for the analysis of minerals and/or detection of heavy metal poisons in hair.[62] The authors attempted to compare the results of the CF-LIBS-calculated concentrations with results obtained from a commercial analytical laboratory utilizing ICP-MS. The CF-LIBS analysis required only a few mm of hair and took less than two minutes to determine the entire elemental content. The authors observed a variation of the "matrix-effect" by measuring differences in plasma temperature and more drastic differences in electron density for subjects of different hair colors (black, brown, or gray). The authors noted that specimens with identical elemental concentration may yield different LIBS spectra due to the variation in temperature and electron density. They concluded that care must be taken during hair analysis to account for variations in measured compositions between subjects with different hair color. Presumably similar effects may be observed in tests utilizing different color skin specimens, although no study has yet measured this. The authors calculated Na/K and Na/Mg ratios that agreed with the ICP-MS measurements within the measurement errors of the two techniques.

4. ANALYSIS OF BIOMEDICAL SPECIMENS.

4.1 Introduction

In this section, we will describe the work that has been conducted on the use of LIBS as an analytical technique for biomedical (fluid) specimens, such as blood, urine, saliva, and the characterization of proteins and amino acids in such fluid specimens. Fluid analyses are typically conducted by commercial or hospital laboratories with a significant turn around time that could perhaps be alleviated by the use of a rapid LIBS testing protocol. For example, blood specimens may be tested with the Comprehensive Metabolic Panel (CMP) or "chem 12" panel which tests for, among other things, calcium, total protein, sodium, potassium, chloride, and alkaline phosphate or a "renal panel" which tests for, among other things, sodium, potassium, phosphorus, glucose, chloride, CO_2, and calcium. Many of these elements or compounds may be quickly and inexpensively quantifiable via the elemental LIBS spectrum.

4.2 Blood

To investigate this possibility, Melikechi et al. performed preliminary tests on specimens of whole blood to determine the resulting LIBS emission spectrum. Spectra in the region 200-970 nm were obtained from solid frozen mouse blood tested in a helium environment with a nanosecond 1064 nm LIBS system.[63] The authors observed that nearly 90% of the peaks below 300 nm were due to carbon and iron alone, most likely due to iron's large number of UV emission lines and its important role in hemoglobin. They also observed lines of Ca, Mg, Na, O, K, N, and H. No attempt was made to quantify the concentrations of these elements in the blood samples.

4.3 Proteins

Melikechi et al. also tested water solutions of proteins relevant to cancer research.[63] Using the same apparatus described earlier, they utilized a principal component analysis (PCA) to differentiate the LIBS spectra obtained from water solutions of bovine serum albumin, insulin-like growth factor II, and leptin. The results demonstrated that not only can good signal-to-noise LIBS spectra be obtained from solutions of proteins and their organic molecules, but that sufficient differences exist in the LIBS spectra obtained from these solutions to allow their classification by an appropriate multivariate chemometric technique. The limits of detection of this technique are not known, and no protein concentrations were provided.

An amino acid is an organic molecule comprising a protein. Chinni et al. used a nanosecond Nd:YAG LIBS system to analyze residues of amino acids on swipes by focusing the LIBS laser to a line focus on three swipe materials.[64] By manually rubbing the swipe material into pure specimens of high-purity powdered L-asparagine ($C_4H_8N_2O_3$) and L-leucine ($C_6H_{13}NO_2$), a thin film of residue was created on the swipe.

The authors utilized a "whole spectrum" chemometric algorithm, utilizing all 37,220 intensity channels as independent variables in a partial least squares regression in combination with principal component analysis (PLS2) to differentiate the spectra from the two proteins. Using the best or strongest LIBS spectra to create a model with this algorithm and the worst spectra to test this model, the authors observed differentiation of the proteins from each other as well as the "clean" swipe material. It is significant that

the LIBS elemental assay can differentiate these powders, as the elemental composition of the amino acids is the same (C, H, N, and O), only their stoichiometries are different.

5. ANALYSIS OF MICROORGANISMS CAUSING HUMAN DISEASE.

5.1 Introduction

Significant research effort has been expended in the area of LIBS-based pathogen identification. Pathogens are a loosely defined group of microorganisms that can infect a human host including bacteria, viruses, molds, prions, amoebae, and fungi. Because of their ubiquity and their impact on human health, there is a well-recognized need for new diagnostic technologies that can rapidly identify pathogenic bacteria without an *a priori* knowledge of nucleic acid sequences (required for polymerase chain reaction (PCR) techniques) or antibodies against known bacterial antigens (which fluorescence immuno-assay techniques require). Numerous research efforts have been initiated worldwide to investigate if the speed and lack of sample preparation that a LIBS-based analysis offers can fill this role.[14]

As well as their importance to human health, the size and mass of a bacterial cell (on the order of 1 μm, corresponding to a cell mass of 1 pg) [65] make bacterial pathogens more appropriate for LIBS analysis than viral pathogens, which have a mass approximately 1000 times smaller. Chaleard et al. have measured the mass of Al ablated per laser pulse to be in the range of 200-400 ng,[66] therefore the bacterial mass offers a better possibility of providing a reasonable signal to noise analytical signal when a clinically realistic number of bacterial cells are ablated. In fact Dixon and Hahn have observed useful diagnostic signal from individual *Bacillus atrophaeous* spores, detecting an average measured calcium mass per laser pulse of 3.1 fg.[67] Other authors have obtained useful analytic signals from similarly sized bioaerosals.[68,69]

5.2 Bacterial pathogens

Beginning in 2003, and partially motivated by the *Bacillus anthracis* "anthrax" bioterrorism attacks of 2001, multiple proof-of-concept experiments were conducted to show the ability of LIBS to rapidly detect harmful Gram-negative and Gram-positive bacteria and spores.[70,71,72,73,74,75,76] Limitations of these early tests included the use of unrealistic freeze dried powders or pellets (lyophilized cells), the use of a very limited number of species focused on spore-form *Bacilli* (e.g. *Bacillus subtilis* var. *niger* commonly referred to as *Bacillus globigii*), and the lack of chemometric analysis to discriminate highly similar spectra. Nonetheless, all initial tests demonstrated the ability to differentiate the LIBS spectrum acquired from pathogens of interest from other similar spectra, particularly naturally occurring background biological "confusants" or "interferents" such as pollens or molds. In all cases, this discrimination was based on the observed optical emission strength of inorganic elements present in the microorganism. This is shown in Figure 6.

From 2006-2007, Baudelet et al. reported more in-depth investigations into the use of LIBS for rapid bacterial identification. Specifically, the use of both nanosecond and femtosecond laser pulses was investigated on five different species of bacterium, including *Acinetobacter baylyi*, *Bacillus subtilis*, *Erwinia chrysanthemi*, *Escherichia coli*, and *Shewanella oneidensis*.[77,78] Genus-level discrimination was observed by using

the emission intensity of elements present in the bacterial cell: Na, Mg, P, K, Ca, and Fe. The advantages of using a femto-LIBS apparatus were noted, specifically the observation of intense molecular CN band emission (relative to atomic carbon emission).[79] Intriguingly, the time-evolution of the intense CN band differed in plasmas formed from the ablation of organic (bacterial) targets compared to abiotic pure graphite targets, allowing a quantification of the native molecular composition of the ablated target. This result has been confirmed using nanosecond UV pulses.[80]

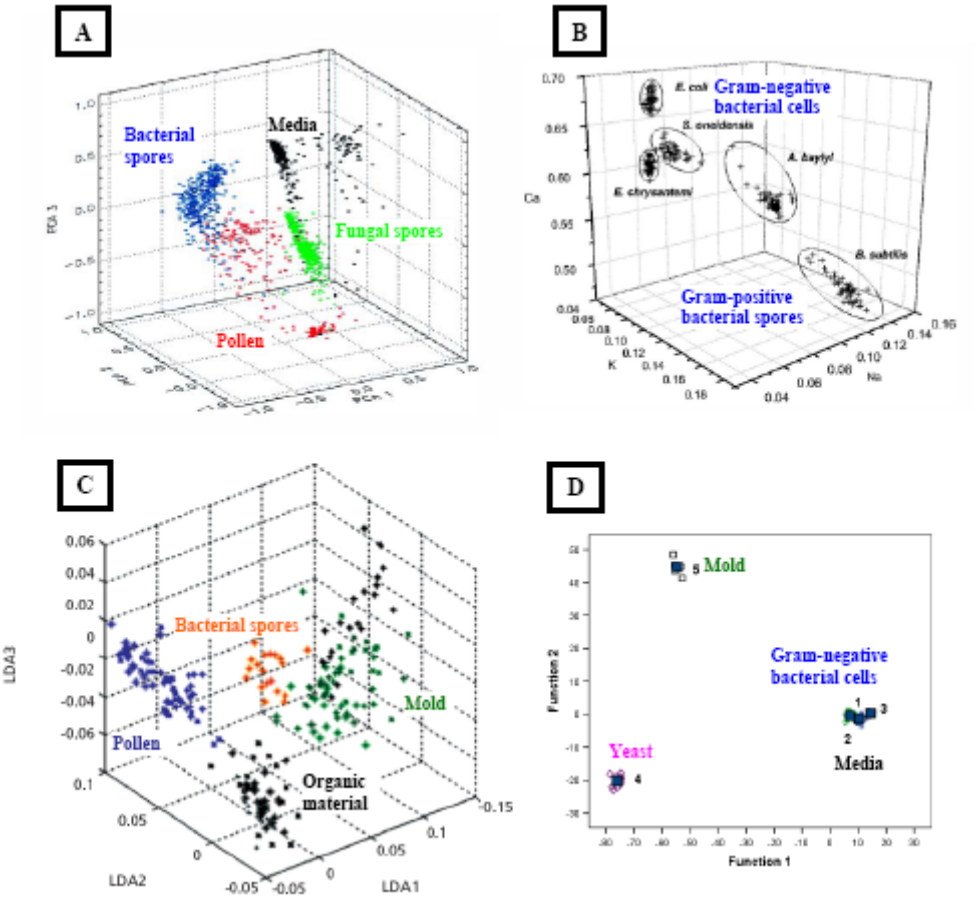

Figure 6. A LIBS-based elemental analysis of microorganisms allows discrimination between multiple biotypes, including bacteria, pollen, mold, fungi, and yeast. (*A*) The first three principal components of a principal component analysis were able to differentiate bacteria, fungi, pollen, and a nutrient medium used to culture the microorganisms (*adapted from ref. 72*). (*B*) Discrimination was easily observed between Gram-negative bacteria and Gram-positive spores in a trace element hyperspace classification on the basis of their Ca, K, and Na content (*adapted from ref. 77*). (*C*) The first three scores in a linear discriminant analysis were able to provide discrimination between Gram-positive bacterial spores, pollen, mold, and other organic materials such as starch and egg albumin (*adapted from ref. 83*). (*D*) The first two discriminant function scores provided discrimination in a discriminant function analysis between specimens of yeast, mold, and Gram-negative bacteria (*E. coli*), as well as the nutrient medium on which they were cultured (*adapted from ref. 89*).

The use of femtosecond laser pulses also opens up a greater possibility of remote detection and sensing of harmful pathogens due to the formation of intense femtosecond "filaments" due to Kerr-effect self-focusing. Such filaments can propagate over great

distance with little loss of intensity and no defocusing, allowing the ablation of biological targets at variable distances. Although this has not been performed on pathogenic targets, adequate signal-to-noise measurements have been made on biological targets at distances up to 32 m.[81,82]

In 2007 Merdes et al. addressed the issue of discriminating a bacterial target (*B. subtilis* spores) from non-pathogenic biological confusant targets such as pollens, molds, starch, and egg albumin when tested on a background of cleaned or painted metal. Utilizing an automated software package in MATLAB which consisted of spectral preprocessing of a 2048 channel spectrum and a principal components analysis followed by a linear discriminant analysis of the first 11 principal components, they were able to demonstrate classification of the bacterial targets with false-positive and false-negative performances of 1% and 3%, respectively.[83]

Building on the work of Merdes, researchers affiliated with the United States Army Research Laboratory focused on developing the hardware and the chemometric algorithms necessary for identifying residues of harmful agents, including pathogenic bacteria, when ablated in the presence of an unknown background substrate. Recognizing that the key to any pathogen identification is the construction of an appropriate chemometric model algorithm, they investigated multiple linear regression and neural network analysis models to differentiate a bacterial (*Bacillus atrophaeus*) and a biological (ovalbumin) spectrum from an array of potential interferent compounds (mold spores, humic acid, house dust, and Arizona road dust).[84] Using a 1064 nm nanosecond LIBS system, they measured false negative rates of 0% for spectra obtained from 100 colony forming units of the bacteria.

At the same time, use of a double-pulse stand-off LIBS system was demonstrated to record high signal-to-noise LIBS spectra from targets of *Bacillus globigii* and mold (*Alternia alternate*) at a distance of 20 m.[85] At this point the use of increasingly complex algorithms to discriminate the similar spectra acquired from microorganisms began to show efficacy. Single shot LIBS spectra from residues of *Bacillus globigii* and the ricin surrogate ovalbumin (ova) were obtained from dried powders of the samples fixed on doublesided adhesive tape.[86] Using a partial least squares discriminant analysis (PLS-DA) the authors showed how the selection of variables used to create the PLS-DA model was extremely important in order to avoid over-fitting the model and to maximize the predictive power of the model. At the present time, this is still an active area of investigation, and it is not yet apparent if a set of independent variables comprised of the entire LIBS spectrum or a carefully pre-selected sub-set or sub-sets of the spectrum containing only important atomic emission lines (called "variable down-selection") is preferable for optimal discrimination. Nonetheless, they have shown that either is preferable to the use of simple atomic emission line intensities in the case of complex spectra. In fact, by carefully constructing PLS-DA models and appropriately choosing the down-selected variables in the dense LIBS spectra from organic targets, Gottfried has shown excellent discrimination of *Bacillus atrophaeus* spores, *E. coli*, MS-2 bacteriophage, α-Hemolysin, and *Staphylococcus aureus* using a compact portable LIBS system with a 25-mJ 1064 nm nanosecond laser. This was demonstrated even when the target was placed on a variety of background substrates that also contributed to the spectrum (aluminum, steel, or polycarbonate) and when mixed with a host of similar confusant materials (such as ova and lime).[87]

Recently, this work has been expanded upon by Cisewski et al. who investigated the use of a support vector machine chemometric algorithm to classify spectra obtained from bulk powder pellets of *Bacillus atrophaeus*, *Bacillus cereus* (ATCC 14603), *Bacillus thuringiensis* (ATCC 51912), and *Bacillus stearothermophilus* (ATCC 12979) along with a variety of powdered confusant materials.[88] Efficient classification (a predication error of 3.3% for the spore powders) was shown using all 13,701 spectral intensity channels.

During the same time, our group was concentrating more on the microbiological aspects of a LIBS-based pathogen identification diagnostic test. The philosophy of these experiments was to perform analyses on bacterial specimens of interest to the medical community under clinically relevant conditions. This included testing live bacteria from a variety of Gram-positive and Gram-negative species grown under a variety of conditions, although this list is still far from complete. Initially, a discriminant function analysis revealed reproducible differences in the spectra obtained from four strains of *E. coli* (including the pathogen enterohemorraghic *E. coli* or O157:H7), an environmental mold, and the *Candida albicans* yeast.[89,90] The spectra were obtained using a nanosecond 1064 nm LIBS system with testing done in air. As well, the first test on bacterial specimens cultured using different nutrition media (a solid tryptic soy agar and a liquid tryptic soy broth) was performed, showing that differences in a cell's nutritional environment during cell reproduction do not impede LIBS classification. The intensities of 19 observed atomic emission lines normalized by the total spectral power were used as independent variables in these DFAs. This result was confirmed with specimens of the Gram-negative *Pseudomonas aeruginosa* cultured on three solid media: tryptic soy agar, blood agar, and MacConkey agar, which were easily discriminated from the *E. coli* spectra and from pure samples of the growth media.[91] Some alteration of the LIBS spectrum from bacteria cultured in the MacConkey medium was observed and attributed to a not-unexpected membrane interaction with the deoxycholate present in the medium, a known detergent for lipid membranes. This result was confirmed in 2011 by Marcos-Martinez et al. who also tested *E. coli* and *P. aeruginosa* as well as *Salmonella typhymurium* on three solid nutrition media, adding a *Brucella* anaerobic agar to the test.[92] Using a neural network analysis of their 2048 channel spectrum, they demonstrated 100% bacterial strain identification regardless of growth medium.

After these initial tests we began ablating all bacterial specimens in an inert argon environment, although both argon and helium were investigated.[93] Repeated measurements of Gram-negative bacteria on a variety of media, including media specifically created to induce outer membrane elemental alteration, revealed that changes in the calcium and magnesium concentration in the bacterial cell, specifically in the outer membrane, can be monitored with the LIBS spectrum.[94] For the Gram-negative bacterium, the outer membrane is first and foremost a permeability barrier. But primarily due to its polysaccharide content, it possesses many of the interesting and important characteristics of the Gram-negative bacterial cell.[95,96] The outer face of the outer membrane may contain some phospholipids, but mainly it is formed by a different type of amphilic molecule which is composed of lipopolysaccharide (LPS).[97,98] In the outer membrane two specific divalent cations, Ca^{2+} and Mg^{2+}, play a crucial role in stabilizing the membrane by binding adjacent LPS molecules.[99] The exact mechanism of the stabilization of the cations is not completely clear, but changes in membrane permeability

as a function of cation concentration (Ca, Mg, Na, and Ba) have been observed and are directly related to antibiotic efficacy against the bacteria.[100,101] It is these specific cations to which LIBS is particularly sensitive on the basis of their intense easily observed atomic emission lines and it is these cation concentrations that we have observed changes in when cells were exposed to known membrane detergents. This connection between the LIBS assay and the membrane composition suggests a possible serological (surface antigen-based) description of the LIBS-based identification.

The effect of "mixed cultures" (two or more bacterial types in one specimen) was studied by preparing two-component bacterial mixtures (*Mycobacterium smegmatis* and *E. coli*) of known mixing fraction. The majority bacterial species was correctly identified by a DFA when it constituted more than 80% of the mixture and the identification accuracy dropped quickly for mixing fractions below 80%, achieving the anticipated 50% level for 50:50 mixtures.[102] We later reproduced this result in mixtures of *E. coli* (ATCC 25922) and *Enterobacter cloacae* (ATCC 13047) to simulate specimen contamination in a clinical pathology laboratory.[103] We have also shown that a LIBS-based bacterial identification is independent of bacterial titer by showing that serial dilutions of a strain of *M. smegmatis* were correctly discriminated 100% of the time from a second strain of *M. smegmatis* regardless of cell titre, although the analytic LIBS signal intensity demonstrated linear dependence with cell count.

We then initiated a series of tests to replicate clinically relevant conditions. We investigated the effect that a variety of environmental and metabolic stresses might have on the bacterial LIBS spectrum. We obtained spectra from approximately 7500 bacterial cells of *E. coli* (strain C) that were exposed to bactericidal ultraviolet radiation and a second specimen that had been autoclaved, rendering both specimens completely safe.[104] 100% of test spectra from *E. coli* treated in both ways were classified correctly in a model containing a second strain *E. coli* (ATCCC 25922) and a specimen of *M. smegmatis*. Importantly we demonstrated no loss of signal in the UV exposed specimens, indicating that biohazardous samples may first be inactivated by UV irradiation, rendering them significantly safer for handling. To prove efficacy in multiple phenotypes, identical results were shown for the Gram-positive *Streptococcus viridans*.

We then studied the effects of deposition on a nutrient-free abiotic surface by placing specimens in an isolated 21°C environment. LIBS spectra were not altered in any measureable manner in specimens of *S. viridans* and *E. coli* (strain C) when they were acquired up to nine days after mounting on the abiotic surface. It should be noted that these specimens did not die during this starvation trial, but would have entered a dormant, non-reproducing state. These bacteria were "viable, but non-culturable," and thus undetectable by most modern methods.[105] At no point was any specimen, no matter what stress it was exposed to, classified as anything other than its correct identity.

We have shown that the presence of minerals and salts in sterile urine do not hinder a LIBS-based bacterial identification. Aliquots of *Staphylococcus epidermidis* were harvested from sterile urine specimens and tested without washing or any sample preparation and were correctly identified 100% of the time by a DFA model containing no urine exposed spectra.[103] The model contained only our standard library spectra of *S. epidermidis* (from water aliquots) as well as two other species of Staphylococci, including *S. aureus* and *S. saprophyticus*. Lastly we have shown excellent genus-level discrimination capabilities of the LIBS-based identification using a DFA model

containing spectra obtained from five different genera and 13 classifiable taxonomic groups of species and strains. This is shown in Figure 7. Truth tables constructed from an external validation test of the five genus model shown in Figure 7(a) yielded sensitivities of approximately 85% and specificities above 95% with a testing set of over 600 bacterial spectra.[103]

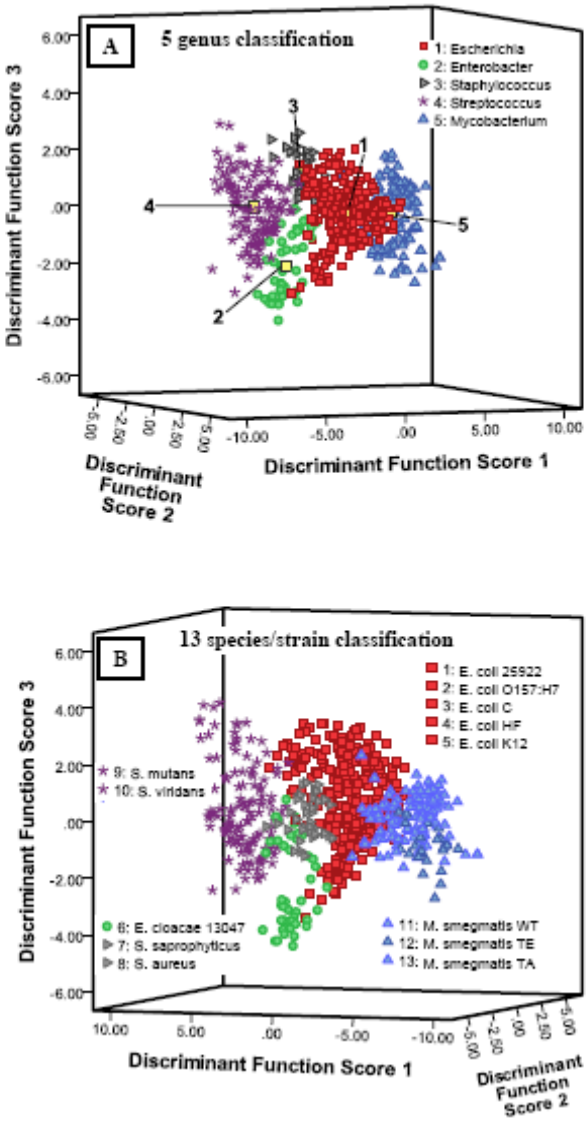

Figure 7. The first three discriminant function scores of a DFA performed on 13 elemental emission lines in the LIBS spectra from live bacterial specimens. Sensitive and specific discrimination/classification of bacterial pathogens and non-pathogenic bacteria was observed in external validation tests performed with these two models. (*A*) The bacterial specimens were grouped by genus in the model showing the possibility of a rapid genus-level identification of an unknown sample utilizing the LIBS spectrum. (*B*) Thirteen bacterial classes of strain and species were left ungrouped and no association between samples was provided to the model. The natural clustering of the classes by species and genus demonstrated that there were reproducible and consistent elemental differences in the bacterial cell which can be quantified by the LIBS assay and used as a basis for identification of unknown specimens. (*A and B adapted from ref. 103*).

Strain-level identification has also been shown by Multari et al. who differentiated specimens of *E. coli*, three clonal methicillin-resistant *Staphylococcus aureus* (MRSA) strains, and one unrelated MRSA strain with a 1064 nm nanosecond LIBS system.[106] These authors utilized an algorithm based on a sequential projection to latent structures (PLS) regression model constructed from the whole spectrum (205 to 1000 nm) constituting 39,730 variables. They also suggested and put into practice a sequential "flow-chart" style algorithm that identified an unknown spectrum by sequentially testing it in a series of "yes" or "no" classification tests, each one typically discriminating between groups with progressively less variance in the data. In 2012 this group expanded on this technique, demonstrating bacterial classification of specimens of *Bacillus anthracis* Sterne strain mounted as a bacterial lawn on blood agar, dilutions on agar, and dilutions on glass.[107] This study was conducted at a standoff distance inside a biosafety cabinet and the PLS model was constructed with 4096 independent variables from the entire spectral range (237–1015 nm).

Progress is being made on using LIBS analyses to detect/identify pathogens relevant to food safety such as *E. coli*, which is a common meat contaminant [90,91,108] and *Salmonella enterica*, a common Gram-negative foodborne pathogen. Using the fourth harmonic (266 nm) of a nanosecond LIBS system, Barnett et al. demonstrated efficient identification of *Salmonella enterica* serovar Typhimurium in various liquids such as milk, chicken broth, and brain heart infusion.[109] A comparison of the LIBS assay with a polymerase chain reaction (PCR) assay of *S. enterica* showed that the LIBS assay is currently not as sensitive as PCR (because there is no amplification step), but it was still able to detect bacterial titers above 10^5 cfu/mL. Alternatively, we have shown that if sufficiently concentrated, sensitive identification can be performed with as few as 2500 cells.[102]

Although non-medical, Lewis et al. have made a significant contribution to the development of the technique by showing that a femtosecond LIBS system can be used to differentiate and discriminate between bacteria reclaimed from various bauxite soils, which is similar to unknown bacteria being obtained from various foods or clinical specimens via washing or swipes.[110] They concluded that femto-LIBS can indeed be utilized to not only discriminate bacteria based on where they were obtained (due to harsh and fluctuating chemical environments) but that it can also differentiate both bacterial species and strain.

5.3 Viral Pathogens

Due to their low mass, viruses have not yet been a common target for LIBS biomedical assays. In 2012 Multari et al. tested four strains of UV-killed hantavirus that had been diluted in liquid iodixanol and plated on glass slides.[107] No determination was made of the number of viruses tested, but discrimination of the strains was observed after construction of an appropriate PLS regression model (again performed sequentially) that necessarily contained the iodixanol and the glass slide.

5.4 Molds, pollens, amoeba

The other pathogens have not received the level of interest that the bacteria have received. Because pathogens such as molds, fungal spores, and pollen spores were tested in the broader context of bacterial biosensing, it is not necessary to reiterate all the

relevant details here, as all the pertinent conclusions have been discussed in section 5.2. Among the list of such infectious bioagents which have been shown to be easily differentiable from bacteria by virtue of their LIBS spectrum are: molds,[71,72,83,85,86,89] pollens,[68,70,71,72,83] yeast,[89] and fungal spores.[72]

6. LIBS-GUIDED SURGERY

6.1 Laser-guided surgery

One last medical application of LIBS remains to be covered, and that is the use of the visible wavelength emission spectrum produced during ablation as a real-time monitor of surgical progress. Much as it has been suggested in section 2.3 that the differences in the LIBS spectrum from caries and healthy dental tissue can prove a dentist with a way of monitoring tooth-drilling progress, it is believed that a similar optical feedback can be used to guide the surgeon utilizing a laser scalpel or a cardiologist performing laser angioplasty.

It has been known for some time that laser ablation with pulsed lasers at a variety of wavelengths can provide an effective method of cutting through tissues during medical procedures [111] although the physical mechanisms that govern ablation, plasma formation, and tissue disruption can be quite complicated and have been studied extensively.[112,113,114] While many of the early studies cited above investigated the physical characterization of pulsed laser drilling, cutting, or ablation as they pertain to medical procedures, it was not immediately recognized that the light emitted during the ablation process (often called plasma emission luminescence) could be used as a means of providing optical feedback to the operator.[115,116] In fact, it is still well known that,

> "*…the surgeon gets no feedback during laser ablation. There is no depth sensation and no tissue specificity with a laser incision…Future prospects may solve these problems by means of an optical feedback mechanism that provides a tissue-specific laser ablation.*"[117]

The recent work to characterize the tissue-specific emission observed in the LIBS plasma described in sections 2 and 3 has attempted to address this issue, but has not gained significant traction within the broader medical community. As early as 1998 Kim et al. suggested a method for utilizing the observed "plasma luminescence spectrum" as a way of monitoring laser ablation in the vicinity of bone and the spinal cord.[115] They observed that the total emission intensity decreased with depth, but the ratio of two wavelength channels, one analyte and one normalization, remained constant as a function of depth and acted as a suitable feedback control signal. Of course, the use of any of the numerous chemometric algorithms already described in this chapter to classify the entire LIBS spectrum would provide an even greater real-time feedback of tissue composition.

As well as determining the tissue composition, multiple optical modalities may be combined with LIBS in a single endoscopic instrument, such as the use of laser light to measure the distance from the end of the scope to the tissue to better than 1 mm.[118] The scheme suggested by Kim [115] was implemented by Jeong et al. in 2012 during surgery on a mouse skull that demonstrated a precision LIBS-guided craniotomy utilizing an ultrafast (100 fs) Ti:sapphire ablation laser.[119] This is shown in Figure 8.

Although the ablation laser was not delivered through an optical fiber in this study, the use of optical fiber for both laser pulse delivery and optical emission

collection, both with and without inert gas co-delivery (similar to an endoscopic procedure), has been shown in numerous applications including the characterization of completely submerged targets.[120,121,122,123,124] This use of a fiber for laser delivery and light collection has not yet been demonstrated in a medical *in vivo* or *ex vivo* procedure.

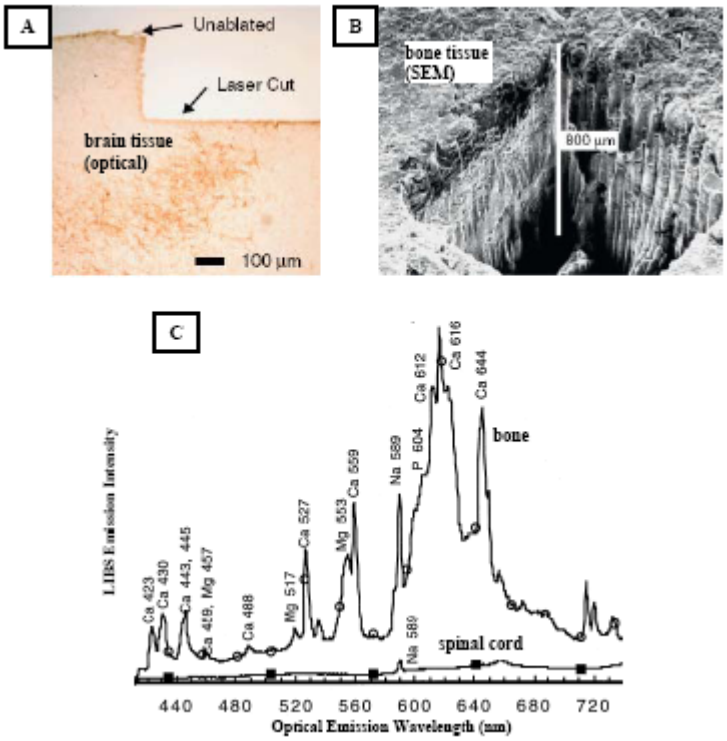

Figure 8. A LIBS-guided surgical procedure to cut through the skull without damaging underlying brain tissue. (*A*) A bright-field optical micrograph of cross-sectioned rat brain tissue laser-ablated under saline (*adapted from ref. 119*). (*B*) A scanning electron micrograph of porcine bone tissue laser-ablated in air (*adapted from ref. 119*). Note the difference in scale between A and B. (*C*) The LIBS optical emission spectra from bone (top) and spinal cord (bottom) tissues ablated in air with the strongest observed emission lines in each identified (*adapted from ref. 115*). The spinal cord possessed a significantly different spectrum than the bone, allowing a cutting procedure to be terminated when the observed bone emission spectrum changed. All data acquired using ultrafast femtosecond Ti:sapphire ablation.

Despite the demonstration of sensitive and specific tissue classification during LIBS procedures and the fabrication of suitable experimental schemes for LIBS-guided surgery, it still remains true that,

> "*No device currently exists that combines the cutting capability of plasma-mediated ablation, using ultra-short laser pulses to ensure negligible collateral tissue damage, with feedback control of the cutting process.*"[119]

It is clear, therefore, that areas of future experimentation will by necessity combine a medical expertise in laser surgery and cutting with the expertise in performing LIBS on tissues and analyzing and/or classifying the LIBS spectral data in real-time. A

greater number of interdisciplinary collaborations conducting experiments in medical research facilities or the hospital operating theatres will be required.

6.3 Future potential

Alternate schemes for monitoring tissue composition during ablation include diffuse reflectance spectroscopy (DRS),[125] two-photon fluorescence,[126] and Raman spectroscopy,[127] among others. However, none of these methods directly analyze the ablation process itself, instead utilizing a second source of illumination to sample the tissue after ablation and prior to the next laser pulse. The use of LIBS-guided surgery offers the only possibility of true real-time feedback of the cutting process. It is not inconceivable however that one or more optical imaging modalities may be incorporated into the endoscope or laser scalpel to provide full characterization of the tissue, in addition to the LIBS analysis of the ablation plasma. The combination of multiple spectroscopic modalities, including LIBS, with the use of sophisticated chemometric algorithms has not been incorporated yet into such a surgical instrument and offers an exciting possibility for highly sensitive tissue discrimination, especially given the numbers of demonstrations of *ex vivo* tissue classification already performed.

Additionally, the use of fiber lasers as the ablation source to replace the bulky and power-intensive pulsed YAG lasers is gaining popularity and is an advancement that could hasten the integration of the LIBS technique into medical endoscopic or surgical devices.[128] Such fiber lasers, now becoming commercially available, offer a high quality beam capable of delivering enough energy to generate the LIBS plasma while operating at high repetition rates. These lasers come in a quite compact package consuming relatively low amounts of wall-plug power (due to their high efficiency) while generating significantly lower amounts of excess heat. Importantly, as demonstrated by Baudelet et al. in 2010, the use of a fiber laser such as an actively Q-switched Tm^{3+}-doped fiber laser operating at 2 μm is gaining attention for medical laser ablation because the 2 μm laser wavelength overlaps with several water absorption peaks, providing superior tissue ablation and cutting.[129] The incorporation of such a laser into a medical endoscopic tool has not yet been investigated.

It is clear that there exists a great future potential for the application of LIBS in a wide variety of medical and biomedical applications. Numerous early results have already confirmed the utility and efficacy of this approach, and future advances in hardware and software for real-time spectral analysis will only increase the utility of the technique. As medicine moves toward a more information-guided paradigm, where patient treatments and procedures are predicated on and guided by real-time diagnostic point-of-care information, obtained easily and non-invasively if possible, the information provided by a LIBS analysis could constitute a very important contribution.

1

[1] S.A. Kane, *Introduction to Physics in Modern Medicine*, 2nd edn. (CRC Press, New York, 2009), pp.77-81

[2] G.R. Kulkarni, Bull. Mater. Sci. **11**, 239 (1988)

[3] K.D. Solomon, L.E. Fernández de Castro, H.P. Sandoval, J.M. Biber, B. Groat, K.D. Neff, M.S. Ying, J.W. French, E.D. Donnenfeld, R.L. Lindstrom, Ophthalmology **116**, 691 (2009)

[4] T.S. Das, J. Endovasc. Ther. **16** (Suppl II), II98 (2009)

[5] L.I. Deckelbaum, Lasers Surg. Med. **14**, 101 (1994)

[6] M. Wanner, Dermatol. Ther. **18**, 209 (2005)

[7] M.A. Adatto, Med. Laser Appl. **19**, 175 (2004)

[8] M.L. Walter, M.E. Domes, R.A. Diller, J. Sproedt, U.H. Joosten, Lasers Surg. Med. **25**, 153 (1999)

[9] J.A. Burns, A.D. Friedman, M.J. Lutch, R.E. Hillman, S.M. Zeitels, J. Laryngol. Otol. **124**, 407 (2010)

[10] J.M. Brunetaud, V. Maunoury, P. Ducrotte, D. Cochelard, A. Cortot, J.C. Paris, Gastroenterology **92**, 663 (1987)

[11] F.C. Holsinger, A.D. Sweeney, K. Jantharapattana, A. Salem, R.S. Weber, W.Y. Chung, C.M. Lewis, D.G. Grant, Curr. Oncol. Rep. **12**, 2162 (2010)

[12] V.K. Singh, A.K. Rai, Lasers Med. Sci. **26**, 673 (2011)

[13] A.K. Pathak, R. Kumar, V.K. Singh, R. Agrawal, S. Rai, A.K. Rai, Appl. Spectrosc. Rev. **47**, 14 (2012)

[14] S.J. Rehse, H. Salimnia, A.W. Miziolek, J. Med. Eng. Technol. **36**, 77 (2012)

[15] H.H. Telle, O. Samek, in: *Laser-Induced Breakdown Spectroscopy*, ed. by I. Schechter, V. Palleschi, A.W. Miziolek (Cambridge University Press, Cambridge, 2006), pp. 282-313

[16] F.H. Loesel, M.H. Niemz, J.F. Bille, T. Juhasz, IEEE J. Quant. Elec. **32**, 1717 (1996)

[17] O. Samek, D.C.S. Beddows, H.H. Telle, J. Kaiser, M. Liska, J.O. Caceres, A. Gonzales Urena, Spectrochim. Acta B **56**, 865 (2001)

[18] A. Hrdlička, L. Prokeš, A. Staňková, K. Novotný, A. Vitešníková, V. Kanický, V. Otruba, J. Kaiser, J. Novotný, R. Malina, K. Páleníková, Appl. Opt. **49**, C16 (2010)

[19] O. Samek, D.C.S. Beddows, H.H. Telle, G.W. Morris, M. Liska, J. Kaiser, Appl. Phys. A **69** [Suppl.], S179 (1999)

[20] O. Samek, M. Liska, J. Kaiser, D.C.S. Beddows, H.H. Telle, S.V. Kukhlevsky, J. Clin. Laser Med. Sur. **18**, 281 (2000)

[21] O. Samek, H.H. Telle, D.C.S. Beddows, BMC Oral Health **1**, 1 (2001)

[22] R.K. Thareja, A.K. Sharma, S. Shukla, Med. Eng. Phys. **30**, 1143 (2008)

[23] V.K. Singh, A.K. Rai, Lasers Med. Sci. **26**, 307 (2011)

[24] Z.A. Abdel-Salam, A.H. Galmed, E. Tognoni, M.A. Harith, Spectrochim. Acta B **62**, 1343 (2007)

[25] Z.A. Abdel-Salam, Z. Nanjing, D. Anglos, M.A. Harith, Appl. Phys. B **94**, 141 (2009)

[26] F.C. Alvira, F. Ramirez Rozzi, G.M. Bilmes, Appl. Spectrosc. **64**, 313 (2010)

[27] A.J. Harding Rains, Ann. Roy. Coll. Surg. Eng. **29**, 85 (1961)

[28] V.K. Singh, V. Singh, A.K. Rai, S.N. Thakur, P.K. Rai, J.P. Singh, Appl. Opt. **47**, G38 (2008)

[29] J. Kuta, J. Machat, D. Benova, R. Cervenka, T. Koristkova, Cent. Eur. J. Chem. **10**, 1475 (2012)

[30] X. Fang, S.R. Ahmad, M. Mayo, S. Iqbal, Lasers Med. Sci. **20**, 132 (2005)

[31] V.K. Singh, V. Rai, A.K. Rai, Lasers Med. Sci. **24**, 27 (2009)

[32] H.S. Kaufman, K.D. Lillemoe, T.H. Magnuson, P. Frasca, H.A. Pitt, Scanning Microscop. **4**, 853 (1990)

[33] M. Ashok, T.R. Rautray, P.K. Nayak, V. Vijayan, V. Jayanthi, S.N. Kalkura, J. Radioanal. Nucl. Ch. **257**, 333 (2003)

[34] K. Proksova, K. Novotny, M. Galiova, T. Vaculovic, J. Kuta, M. Novackova, V. Kanicky, J. Kuta, M. Novackova, V. Kanicky, Chem. Listy **106**, 229 (2012)

[35] A. Wrobel, E. Rokita, P. Thor, Trace Elem. Electroly. **22**, 296 (2005)

[36] T.R. Rautray, K. Dutta, S.L. Das, A.C. Rautray, Nuc. Instrum. Meth. Phys. Res. B **268**, 2773 (2010)

[37] V.K. Singh, A.K. Rai, P.K. Rai, P.K. Jindal, Lasers Med. Sci. **24**, 749 (2009)

[38] A.K. Pathak, V.K. Singh, N.K. Rai, A.K. Rai, P.K. Rai, P.K. Rai, S. Rai, G.D. Baruah, Lasers Med. Sci. **26**, 531 (2011)

[39] J. Anzano, R.-J. Lasheras, Talanta **79**, 352 (2009)

[40] L. Farren, S. Shayler, A.R. Ennos, J. Exp. Biol. **207**, 735 (2004)

[41] F. Marumo, Y. Tsukamoto, S. Iwanami, T. Kishimoto, S. Yamagami, Nephron. **38**, 267 (1984)

[42] E.I. Brima, P.I. Haris, R.O. Jenkins. D.A. Polya, A.G. Gault, C.F. Harrington, Toxicol. Appl. Pharm. **216**, 122 (2006)

[43] I. Pillay, D. Lyons, M.J. German, N.S. Lawson, H.M. Pollock, J. Saunders, S. Chowdhury, P. Moran, M.R. Towler, J. Womens Health **14**, 339 (2005)

[44] A.F. Oluwole, J.O. Ojo, M.A. Durosinmi, O.I. Asubiojo, O.A. Akanle, N.M. Spyrou, R.H. Filby, Biol. Trace Elem. Res. **43-45**, 443 (1994)

[45] Z. Hosseinimakarem, S.H. Tavassoli, J. Biomed. Opt. **16**, 57002 (2011)

[46] M. Bahreini, S.H. Tavassoli, J. Lasers Med. Sci. **3**, 127 (2012)

[47] S. Hamzaoui, R. Khleifia, N. Jaïdane, Z. Ben Lakhdar, Lasers Med. Sci. **26**, 79 (2011)

[48] V. Cirimele, P. Kintz, P. Mangin, Arch. Toxicol. **70**, 68 (1995)

[49] S.V. Campos, M. Yonamine, R.L.M. Moreau, O.A. Silva, Forensic Sci. Int. **159**, 218 (2006)

[50] S. Shadman, M. Bahreini, S.H. Tavassoli, Appl. Opt. **51**, 2004 (2012)

[51] H.P. de Souza, E. Munin, L.P. Alves, M.L. Redígolo, M.T.T. Pacheco, XXVI ENFMC Annal. Opt. **5**, (2003)

[52] M. Adamson, S.J. Rehse, Appl. Opt. **46**, 5844 (2007)

[53] D. Santos Jr., R.E. Samad, L.C. Trevizan, A.Z. deFreitas, N.D. Vieira Jr., F.J. Krug, Appl. Spectrosc. **62**, 1137 (2008)

[54] F.Y. Yueh, H. Zheng, J.P. Singh, S. Burgess, Spectrochim. Acta B **64**, 1059 (2009)

[55] A. Kumar, F.Y. Yueh, J.P. Singh, S. Burgess, Appl. Opt. **43**, 5399 (2004)

[56] J.J. Myers, J.D. Myers, B. Guo, C. Yang, C.R. Hardy, J.A. Myers, A.G. Myers, S.M. Christion, Proc. of SPIE **6863**, 68630W (2008)

[57] Y. Markushin, N. Melikechi, A. Marcano O., S. Rock, E. Henrdon, D. Connolly, Proc. of SPIE **7190**, 719015 (2009)

[58] Y. Markushin, N. Melikechi, in *Ovarian Cancer - Basic Science Perspective*, ed. by S.A Farghaly (InTech, Rijecka, 2012)

[59] A. El-Hussein, A.K. Kassem, H. Ismail, M.A. Harith, Talanta **82**, 495 (2010)

[60] M. Nasiadek, T. Krawczyk, A. Sapoto, Hum. Exp. Toxicol. **24**, 623 (2005)

[61] Q. Sun, M. Tran, B.W. Smith, J.D. Winefordner, Talanta **52**, 293 (2000)

[62] M. Corsi, G. Cristoforetti, M. Hidalgo, S. Legnaioli, V. Palleschi, A. Salvetti, E. Tognoni, C. Vallebona, Appl. Opt. **42**, 6133 (2003)

[63] N. Melikechi, H. Ding, S. Rock, A. Marcano O., D. Connolly, Proc. of SPIE **6863**, 68630O (2008)

[64] R. Chinni, D.A. Cremers, R. Multari, Appl. Opt. **49**, C143 (2010)

[65] H.E. Kubitschek, J. Bacteriol. **172**, 94 (1990)

[66] C. Chaleard, P. Mauchien, N. Andre, J. Uebbing, J.L. Lacour, C. Geertsen, J. Anal. At. Spectrom. **12**, 183 (1997)

[67] P.B. Dixon, D.W. Hahn, Anal. Chem. **77**, 631 (2005)

[68] A.R. Boyain-Goitia, D.C.S. Beddows, B.C. Griffiths, H.H. Telle, Appl. Opt. **42**, 6119 (2003)

[69] D.C.S. Beddows, H.H. Telle, Spectrochim. Acta B **60**, 1040 (2005)

[70] S. Morel, M. Leone, P. Adam, J. Amouroux, Appl. Opt. **42**, 6184 (2003)

[71] A.C. Samuels, F.C. DeLucia Jr., K.L. McNesby, A.W. Miziolek, Appl. Opt. **42**, 6205 (2003)

[72] J.D. Hybl, G.A. Lithgow, S.G. Buckley, Appl. Spect. **57**, 1207 (2003)

[73] N. Leone, G. D'Arthur, P. Adam, J. Amouroux. High Technology Plasma Processes **8**, 1 (2004)

[74] T. Kim, Z.G. Specht, P.S. Vary, C.T. Lin, J. Phys. Chem. B **108**, 5477 (2004)

[75] J.L. Kiel, E.A. Holwitt, J.E. Parker, J. Vivekananda, V. Franz, M.A. Sloan, A.W. Miziolek, F.C. DeLucia Jr., C.A. Munson, Y.D. Mattley, Proc. of SPIE **5795**, 39 (2005)

[76] F.C. DeLucia Jr., A.C. Samuels, R.S. Harmon, R.A. Walter, K.L. McNesby, A. LaPointe, R.J. Winkel Jr., A.W. Miziolek, IEEE Sens. Jour. **50**, 681 (2005)

[77] M. Baudelet, J. Yu, M. Bossu, J. Jovelet, J.-P. Wolf, T. Amodeo, E. Frejafon, P. Laloi, Appl. Phys. Lett. **89**, 163903 (2006)

[78] M. Baudelet, L. Guyon, J. Yu, J.-P. Wolf, T. Amodeo, E. Frejafon, P. Laloi, J. Appl. Phys. **99**, 084701 (2006)

[79] M. Baudelet, L. Guyon, J. Yu, J.-P. Wolf, T. Amodeo, E. Frejafon, P. Laloi, Appl. Phys. Lett. **88**, 06391 (2006)

[80] M. Baudelet, M. Boueri, J. Yu, S.S. Mao, V. Piscitelli, X. Mao, R.E. Russo, Spectrochim. Acta B **62**, 1329 (2007)

[81] H.L. Xu, G. Mejean, W. Liu, Y. Kamali, J.-F. Daigle, A. Azarm, P.T. Simard, P. Mathieu, G. Roy, J.-R. Simard, S.L. Chin, Appl. Phys. B **87**, 151 (2007)

[82] S.L. Chin, H.L. Xu, Q. Luo, F. Théberge, W. Liu, J.F. Daigle, Y. Kamali, P.T. Simard, J. Bernhardt, S.A. Hosseini, M. Sharifi, G. Méjean, A. Azarm, C. Marceau, O. Kosareva, V.P. Kandidov, N. Aközbek, A. Becker, G. Roy, P. Mathieu, J.R. Simard, M. Châteauneuf, J. Dubois, Appl. Phys. B **95**, 1 (2009)

[83] D.W. Merdes, J.M. Suhan, J.M. Keay, D.M. Hadka, W.R. Bradley, Spectroscopy **22**, 28 (2007)

[84] E.G. Snyder, C.A. Munson, J.L. Gottfried, F.C. De Lucia Jr., B. Gullett, A.W. Miziolek, Appl. Opt. **47**, G80 (2008)

[85] J.L. Gottfried, F.C. De Lucia Jr., C.A. Munson, A.W. Miziolek, Spectrochim. Acta B **62**, 1405 (2007)

[86] J.L. Gottfried, F.C. De Lucia Jr., C.A. Munson, A.W. Miziolek, Appl. Spectrosc. **62**, 353 (2008)

[87] J.L. Gottfried, Anal. Bioanal. Chem. **400**, 3289 (2011)

[88] J. Cisewski, E. Snyder, J. Hannig, L. Oudejans, J. Chemometrics **26**, 143 (2012)

[89] J. Diedrich, S.J. Rehse, S. Palchaudhuri, Appl. Phys. Lett. **90**, 163901 (2007)

[90] J. Diedrich, S.J. Rehse, S. Palchaudhuri, J. Appl. Phys. **102**, 014702 (2007)

[91] S.J. Rehse, J. Diedrich, S. Palchaudhuri, Spectrochim. Acta B **62**, 1169 (2007)

[92] D. Marcos-Martinez, J.A. Ayala, R.C. Izquierdo-Hornillos, F.J. Manuel de Villena, J.O. Caceres, Talanta **84**, 730 (2011)

[93] S.J. Rehse, Q.I Mohaidat, Spectrochim. Acta B **64**, 1020 (2009)

[94] S.J. Rehse, N. Jeyasingham, J. Diedrich, S. Palchaudhuri, J. Appl. Phys. **105**, 102034 (2009)

[95] H. Nikaido, *Bacterial Membranes and Walls*, ed. by L. Leive (Marcel Dekker, New York, 1973)

[96] H. Nikaido, T. Takae, Adv. Microb. Physiol. **20**, 163 (1979)

[97] Y. Kamio, H. Nikaido, Biochemistry **15**, 2561 (1976)

[98] C.R.H. Raetz, Ann. Rev. Biochem. **59**, 129 (1990)

[99] L. Leive, Ann. N.Y. Acad. Sci. **235**, 109 (1974)

[100] D.A. Pink, L. Truelstrup Hansen, T.A. Gill, B.E. Quinn, M.H. Jericho, T.J. Beveridge, Langmuir **19**, 8852 (2003)

[101] H.R. Ibrahim, S. Higashiguck, Y. Sugimot, T. Aoki, J. Agric. Food Chem. **45**, 89 (1997)

[102] S.J. Rehse, Q.I. Mohaidat, S. Palchaudhuri, Appl. Opt. **49**, C27 (2010)

[103] Q.I. Mohaidat, K. Sheikh, S. Palchaudhuri, S.J. Rehse, Appl. Opt. **51**, B99 (2012)

[104] Q. Mohaidat, S. Palchaudhuri, S.J. Rehse, Appl. Spectrosc. **65**, 386 (2011)

[105] J.J. Byrd, H.-S. Xu, R.R. Colwell, Appl. Env. Microbiol. **57**, 875 (1991)

[106] R. Multari, D.A. Cremers, J.M. Dupre, J.E. Gustafson, Appl. Spectrosc. **64**, 750 (2010)

[107] R. Multari, D.A. Cremers, M.L. Bostian, Appl. Opt. **51**, B57 (2012)

[108] M. Yao, J. Lin, Q. Li, Z. Lei, L. Huang, Proc. of BMEI 2010, IEEE **302-305** (2010)

[109] C. Barnett, C. Bell, K. Vig, C.A. Akpovo, L. Johnson, S. Pillai, S. Singh, Anal. Bioanal. Chem. **400**, 3323 (2011)

[110] D.E. Lewis, J. Martinez, C.A. Akpovo, L. Johnson, A. Chauhan, M.D. Edington, Anal. Bioanal. Chem. **401**, 2225 (2011)

[111] S. Sato, M. Ogura, M. Ishihara, S. Kawauchi, T. Arai, T. Matsui, A. Kurita, M. Obara, M. Kikuchi, H. Ashida, Lasers Surg. Med. **29**, 464 (2001)

[112] A.A. Oraevsky, R.O. Esenaliev, V.S. Letokhov, Lasers Life Sci. **5**, 75 (1992)

[113] D. Albagli, Dissertation, Massachusetts Institute of Technology (1994)

[114] A.D. Yablon, N.S. Nishioka, B.B. Mikic, V. Venugopalan, Proc. of SPIE **3343**, 68630O (1998).

[115] B.-M. Kim, M.D. Feit, A.M. Rubenchik, B.M. Mammini, L.B. Da Silva, Appl. Surface Sci. **127–129**, 857 (1998)

[116] T. Tong, J. Li, J.P. Longtin, Appl. Opt. **43**, 1971 (2004)

[117] F.W. Neukam, F. Stelzle, Physics Procedia **5**, 91 (2010)

[118] T. Seki, K. Oka, A. Naganawa, H. Yamashita, K. Kim, T. Chiba, Opt. Lasers Eng. **48**, 974 (2010)

[119] D.C. Jeong, P.S. Tsai, D. Kleinfeld, Curr. Opin. Neurobiol. **22**, 24 (2012)

[120] C.M. Davies, H.H. Telle, D.J. Montgomery, R.E. Corbett, Spectrochim. Acta B **50**, 1059 (1995)

[121] O. Samek, D.C.S. Beddows, J. Kaiser, S.V. Kukhlevsky, M. Liska, H.H. Telle, J. Young, Opt. Eng. **39**, 2248 (2000)

[122] D.C.S. Beddows, O. Samek, M. Liska, H.H. Telle, Spectrochim. Acta B **57**, 1461 (2002)

[123] S. Koch, R. Court, W. Garen, W. Neu, R. Reuter, Spectrochim. Acta B **60**, 1230 (2005)

[124] C.E. Dumitrescu, P.V. Puzinauskas, S. Olcmen, Appl. Opt. **47**, G88 (2008)

[125] M.C. Skala, G.M. Palmer, K.M. Vrotsos, A. Gendron-Fitzpatrick, N. Ramanujam, Am. J. Obstet. Gynecol. **186**, 374 (2002)

[126] W.R. Zipfel, R.M. Williams, R. Christie, A.Y. Nikitin, B.T. Hyman, W.W. Webb, Proc. Nat. Acad. Sci. **100**, 7075 (2003)

[127] J.C. Lázaro, A.R. de Paula Jr., L.M. Moreira, J.P. Lyon, M.T.T. Pacheco, C.J. de Lima, Spectroscopy **25**, 147 (2011)

[128] J.-F.Y. Gravel, F.R. Doucet, P. Bouchard, M. Sabsabi, J. Anal. At. Spectrom. **26**, 1354 (2011)

[129] M. Baudelet, C.C.C. Willis, L. Shah, M. Richardson, Opt. Exp. **18**, 7905 (2010)